Talanta 127 (2014) 116–122

Contents lists available at ScienceDirect

Talanta

journal homepage: www.elsevier.com/locate/talanta

# Facile fabrication of a novel anisotropic gold nanoparticle–chitosan–ionic liquid/graphene modified electrode for the determination of theophylline and caffeine

Guangming Yang [a,b], Faqiong Zhao [a,*], Baizhao Zeng [a]

[a] Key Laboratory of Analytical Chemistry for Biology and Medicine (Ministry of Education), College of Chemistry and Molecular Sciences, Wuhan University, Wuhan 430072, PR China

[b] Department of Resources and Environment, Baoshan University, Baoshan 678000, PR China

ARTICLE INFO

*Article history:*
Received 28 November 2013
Received in revised form
11 March 2014
Accepted 13 March 2014
Available online 24 March 2014

*Keywords:*
Gold nanoparticle
Chitosan
Ionic liquid
Theophylline
Caffeine
Electrochemical sensor

ABSTRACT

In the present study, a suspension solution containing anisotropic gold nanoparticle (GNP), chitosan (CHIT) and ionic liquid (IL, i.e. 1-butyl-3-methylimidazolium tetrafluoroborate, [BMIM][$BF_4$]), is prepared by reducing $HAuCl_4$ with sodium citrate in CHIT–IL aqueous solution. The hybrid solution is coated on a graphene (r-GO) modified glassy carbon electrode to construct an electrochemical sensor for the determination of theophylline (TP) and caffeine (CAF). The obtained hybrid film shows rough surface, and anisotropic GNPs are well dispersed on it. The factors concerning this assay strategy are carefully investigated, including the components of the hybrid film, the concentrations of r-GO, $HAuCl_4$ and IL, and the pH of buffer solution. Under the optimized conditions, the linear response ranges are $2.50\times10^{-8}$–$2.10\times10^{-6}$ mol $L^{-1}$ and $2.50\times10^{-8}$–$2.49\times10^{-6}$ mol $L^{-1}$ for TP and CAF, respectively; the detection limits are $1.32\times10^{-9}$ mol $L^{-1}$ and $4.42\times10^{-9}$ mol $L^{-1}$, respectively. The electrochemical sensor shows good reproducibility, stability and selectivity, and it has been successfully applied to the determination of TP and CAF in real samples.



## 1. Introduction

Metal nanomaterials have attracted considerable attention due to their unique optical, electrical, and catalytic properties. Among them, gold nanoparticle (GNP) is the most representative one in electrochemical and biological sensing applications [1–3]. GNP is usually used with other functional materials to fabricate electrochemical sensors, and GNP hybrid films are virtually prepared. There are two traditional approaches to fabricate GNP hybrid films on electrode surface [1,4]. One is to coat electrode surface with GNP suspension containing glutinous agents. The other is electrodeposition. For the former, the dispersion of GNPs is poor, and they agglomerate easily. For the latter, the size and density of GNP heavily depend on electrodeposition time [5]. Small GNP can be acquired by using short electrodeposition time, but the GNP density is usually low. However, when electrodeposition time increases both the size and density of GNP increase [1,5]. Therefore, to fabricate small and dense GNPs decorated hybrid film is still in need of exploration.

Currently, the in situ approach is a promising way to prepare gold nanomaterial because it is usually a one-pot and green process [1]. This approach is based on the reduction of gold salts in the presence of surfactant, organic polymer and IL etc. [5], which regulate the shape and size of nanomaterials and avoid their aggregation or precipitation. For instance, Li et al. used microwave to heat $HAuCl_4$ in 1-butyl-3-methylimidazolium tetrafluoroborate ([BMIM][$BF_4$]) to prepare gold nanosheet [6], and IL was thought to act as the structure-directing agent. Zhu et al. prepared anisotropic GNPs by photochemical reduction of $HAuCl_4$ in [BMIM][$BF_4$], and pointed out that IL was the critical factor for the formation of anisotropic shape [7]. Tsuda et al. fabricated anisotropic GNPs in bis(trifluoromethanesulfonyl)amide anion-based IL using accelerated electron beam irradiation and $\gamma$-ray [8]. These methods are free of additional capping agents, but the reaction conditions are relatively severe. Recently, Yang et al. prepared gold networks@IL ([BMIM][$BF_4$]) by directly reducing $HAuCl_4$ with sodium citrate in [BMIM][$BF_4$] aqueous solution [9]. Similar technologies such as photochemical reduction [4], atmospheric plasma [10] and laser irradiation [11] were also utilized to prepare GNPs using CHIT as the structure-directing agent. In these cases, CHIT was proved to act as a template agent for the formation of anisotropic shape. However, the density of GNPs obtained was low [4,10]. Comparing with physical reduction, the chemical

* Corresponding author. Tel./fax: +86 27 68752701.
*E-mail address:* fqzhao@whu.edu.cn (F. Zhao).

http://dx.doi.org/10.1016/j.talanta.2014.03.029
0039-9140/

method was easy to achieve under simple conditions. For instance, Carlo et al. used organic acids to reduce $HAuCl_4$ in CHIT aqueous solution, and the obtained solution was coated on electrode surface to form CHIT–GNP hybrid film [12]. However, the layout of GNP on electrode surface is agglomerate. There are no reports on the simultaneous application of IL and CHIT to regulate the shape and the size of GNP.

Theophylline (TP) and caffeine (CAF) are important natural alkaloids, and they are usually found in some plants and their products. TP can be used for treating respiratory diseases such as chronic obstructive pulmonary disease and asthma [13], but it also can cause nausea, diarrhea, arrhythmias, etc. [14]. Hence, its use must be monitored to avoid toxicity. CAF is a central nervous system stimulant, and usually used as an additive in energy drinks and soft-drinks, etc. [15]. However, excessive intake of CAF can cause many undesired effects such as cardiovascular disease, depression and hyperactivity [16]. Furthermore, it is a cause of cancer, heart diseases and complications in pregnant women and aging [17]. Therefore, it is necessary to determine the concentrations of CAF and TP in pharmaceuticals, drinks and human physiological liquids, etc.

Hitherto, various methods have been reported for the detection of TP and CAF, including high-performance liquid chromatography (HPLC) [18], gas chromatography [19], spectroscopic methods [20] and electrochemical methods [21–24]. Among these methods, electrochemical methods become popular because of their higher sensitivity, lower cost and faster operation than other methods. However, the electrode surface is crucial for electrochemical determination, which decides the above-mentioned advantages. As a result, various modified electrodes are prepared for the determination of TP and/or CAF, including carbon nanomaterials [21–32], metal nanomaterials [22,33,34], polymer films [35,36] coated electrodes, boron-doped diamond electrodes [37,38] and CdSe microparticles modified electrode [39]. Among them, carbon and metal nanomaterials modified electrodes were widely employed due to their excellent electro-catalytic activity and electron transfer capability. Currently, graphene (r-GO) is the most popular carbon material [40–46], but it has not been used for the purpose.

In this paper, anisotropic GNPs are prepared by reducing $HAuCl_4$ in CHIT–IL aqueous solution. The resulting hybrid solution is directly coated on r-GO modified glassy carbon electrode (GCE) to form a nanocomposite film, which is utilized for the electrochemical determination of TP and CAF. To the best of our knowledge, this is the first time to utilize IL and CHIT to regulate the formation of anisotropic GNP and the shape of hybrid films. The sensor shows high sensitivity, rapid response and low detection limit for TP and CAF.

## 2. Experimental

### 2.1. Apparatus and reagents

All electrochemical experiments were performed with a CHI 617A electrochemistry workstation (Shanghai CH Instruments Co., China). A three-electrode system (10 mL) was used, consisting of a modified glassy carbon electrode as a working electrode, a saturated calomel electrode (SCE) as reference electrode and a platinum foil as counter electrode. Field emission scanning electron microscope (FE-SEM) was performed using a Quanta 450 FEG. Transmission electron microscopy (TEM) was carried out by using a JEM-2100 transmission electron microscope with an accelerating voltage of 200 kV. X-ray diffraction data (XRD) were recorded with a Bruke D8 diffractometer (Germany) using Cu Kα radiation (40 kV, 40 mA) with a Ni filter. An inVia Raman Microscope (Renishaw, Cook, IL) with 514 nm laser was used to determine the quality of graphene on dielectric surface via the characteristic phonon peaks of graphene and they were the averaged data of more than 10 scans sweep from 3000 to 1000 $cm^{-1}$.

Graphene was prepared by a modified Hummers method [47]. Theophylline, caffeine, chitosan (MW: $1 \times 10^6$, 90 to 95% deacetylation), 1-butyl-3-methylimidazolium tetrafluoroborate and chloroauric acid tetrahydrate ($HAuCl_4 \cdot 4H_2O$) were purchased from Sigma (St. Louis, MO, USA). Unless stated otherwise, all other reagents were analytical grade. Tea samples (i.e. Pu'er tea and Green Tea) and energy drink (Red Bull) were purchased from a local supermarket. Theophylline sustained-release tablets (labeled content: 0.1 g per tablet) were purchased from Guangzhou Medtech Xinghua Pharmaceutical Factory Co. Ltd. (China), and Akafen powder (labeled content: 30 mg per tablet) was purchased from Wuhan Zhonglin Pharmaceutical Factory Co. Ltd. (China). The serum and urine samples were obtained from Hospital of Wuhan University without any other treatment and stored at 4 °C. The supported electrolyte was 0.1 mol $L^{-1}$ phosphate buffer solution (PBS), which was prepared with $NaH_2PO_4$ and $Na_2HPO_4$.

### 2.2. Preparation of anisotropic GNP–CHIT–IL hybrid solution

CHIT (0.200 g) was dissolved into 160 mL 0.1 mol $L^{-1}$ acetic acid aqueous solution. Then, 400 μL 25 mmol $L^{-1}$ $HAuCl_4$, 5.00 mL 0.125% CHIT and 25 μL of [BMIM][$BF_4$] were mixed under gentle stirring. Afterwards, the mixed solution was stirred in a three round-bottom flask in oil bath (at 100 °C) for 5 min. After that, 3.0 mL sodium citrate (1%, wt %) was immediately added into above-mentioned solution, and was constantly stirred for 17 min. The solution gradually turned to opaque purple. The formed solution was stored at room temperature for further utilization and characterization. For comparisons, two GNP solutions were prepared under the same conditions except IL–CHIT–water was replaced by water and CHIT–water, respectively. At the same time, five anisotropic GNP–CHIT–IL hybrid solutions were also prepared by changing the concentration of $HAuCl_4$ (i.e. 0.5, 1.0, 2.0, 3.0 and 5.0 mmol $L^{-1}$).

### 2.3. Preparation of anisotropic GNP–CHIT–IL hybrid/r-GO /GCE

Firstly, 1 mg r-GO was dispersed into 1.00 mL DMF to form a suspension (i.e. 1 mg $mL^{-1}$); 5 μL of suspension was coated on a clean GCE surface and dried at room temperature. Then, 5 μL of anisotropic GNP–CHIT–IL hybrid solution was coated on r-GO modified GCE and dried in the air. For each measurement, the electrode was immersed into a blank PBS for successive sweeps of some cycles to regenerate the electrode surface. For comparisons, GO/GCE, r-GO/GCE, CHIT–r-GO/GCE, GNP–CHIT/r-GO/GCE were prepared by changing the components.

### 2.4. HPLC method

HPLC measurements were performed on an Agilent 1100 with a diode-array detector (DAD). Before the measurements, HPLC was calibrated by the solution of the measured compound. And then the content of nonvolatile impurities was calculated by the sum of individual impurities. Here, HPLC was equipped with an ODS-C18 (5 μm × 250 mm) column and DAD detector at 275 nm. The inject volume was 10 μL. The mobile phase was a gradient elution of formic acid/water (0.2%, wt %) and acetonitrile with a flow rate of 1.5 mL $min^{-1}$ [48].

## 3. Results and discussion

### 3.1. Characterization of r-GO

The r-GO was characterized systematically to confirm the production of single or few-layer sheets. Firstly, the powder XRD was used to characterize the bulk structure of the as-prepared r-GO (Fig. S1(A)). A typical broad peak near 10° was observed for the graphene oxide (GO) powder. Compared with GO, the peak of r-GO shifted to 23°, suggesting that r-GO was well ordered two-dimensional sheets with more thorough removal of surface functional groups. Then, the representative Raman spectrum of r-GO was recorded using 514 nm laser irradiations (Fig. S1(B)). The results indicated that the intensity ratio ($I_D/I_G$) of D band and G band was about 1.01, and 2D band indicated that the r-GO had layer structure. Moreover, the morphological characterization of r-GO was investigated by SEM and TEM. The TEM of r-GO powder also showed that r-GO had the single or few-layer sheet (Fig. S1(C)), and when the r-GO was dispersed in ethanol under ultrasonic bath for 30 min, monolayer r-GO was obtained (Fig. S1(D)).

### 3.2. Morphological characterization of modified electrode

The morphology of r-GO and hybrid films is shown in Fig. 1. As can be seen, the r-GO modified GCE exhibits wrinkled structure (Fig. 1(A)). When the reaction is carried out in 0.125% CHIT solution, the obtained film is stacked (Fig. 1(B)) on r-GO/GCE. When both IL and CHIT are present, the obtained hybrid film is similar to that without IL. But with the concentration of IL increasing the hybrid film tends to roll out (Fig. 1(C) and (D)). The result indicates that the concentration of IL can influence the morphology of hybrid film. When the reaction solution contains 5 μL $mL^{-1}$ IL and 0.125% CHIT (Fig. 1(D), the hybrid film has a perfect layout and shows a rough surface. The mechanism for the layout of the hybrid film must remain speculative. According to previous reports [4,7–10,12], IL acts as a capping agent that is selectively adsorbed on a specific crystal surface of GNP. At the same time, CHIT, with a large number of amino and hydroxyl groups, enables the simultaneous synthesis and surface modification of GNP in one pot. Importantly, when the hybrid film is dried on r-GO/GCE, the CHIT is easy to dry and shrink to form agglomerated and stacked shape. On the contrary, IL is difficult to dry and it can prevent the shrink of CHIT. Therefore, we think that the morphology of hybrid film is related to the interaction of GNP, IL and CHIT. The preparation method can overcome the agglomeration of the dropping mixture and produce three-dimensional and mountain-like shape. Thus the hybrid film shows larger surface area than the agglomerated and the smooth one.

Fig. 2 describes the FE-SEM images of different hybrid films prepared on r-GO/GCE. When the hybrid film is prepared with low concentration of $HAuCl_4$ (i.e. 1 mmol $L^{-1}$ in 5 μL $L^{-1}$ IL and 0.125% CHIT solution), the diameters of GNPs are about 50 to 70 nm and GNPs are sparse (Fig. 2(A)). When the concentration of $HAuCl_4$ increases (Fig. 2(B), i.e. 3 mmol $L^{-1}$), the diameters of GNPs become smaller (about 40 to 50 nm), the density of GNP become higher. When the concentration of $HAuCl_4$ is 4 mmol $L^{-1}$, the diameters of GNPs are about 5 to 30 nm (Fig. 2(C)), the density of GNP is high, and the layout of GNP is compact. Comparing with other hybrid film reported [49–51], the small and dense GNPs decorated hybrid film is easy to be obtained.

TEM is also used to investigate the morphology of GNPs prepared with different reaction solutions (Fig. 3). As can be seen in Fig. 3(A), the GNPs are spherical and their diameters are about 30 nm when the reaction is completed in water. When the reaction is performed in CHIT (0.125%) aqueous solution, anisotropic GNPs are obtained, and the diameters are 30 to 50 nm (Fig. 3(B)), indicating that CHIT is a critical factor to make GNP to form an anisotropic structure. When the reaction is performed in CHIT–IL aqueous solution, the diameters of major nanoparticles are 5 to

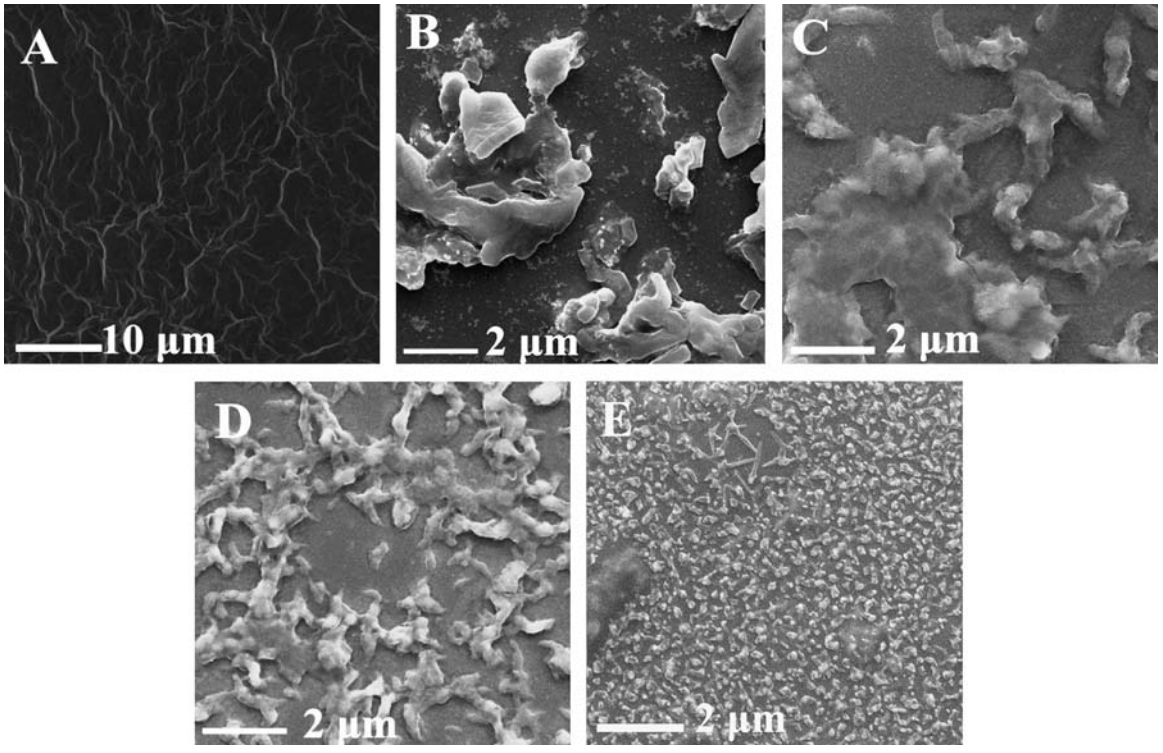


**Fig. 1.** SEM of r-GO and the hybrid films prepared using different concentrations of CHIT and IL. (A) r-GO; (B) CHIT (0.125%, wt%); (C) CHIT (0.125%, wt %) and IL (1 μL $mL^{-1}$); (D) CHIT (0.125%, wt %) and IL (3 μL $mL^{-1}$); and (E) CHIT (0.125%, wt %) and IL (5 μL $mL^{-1}$).

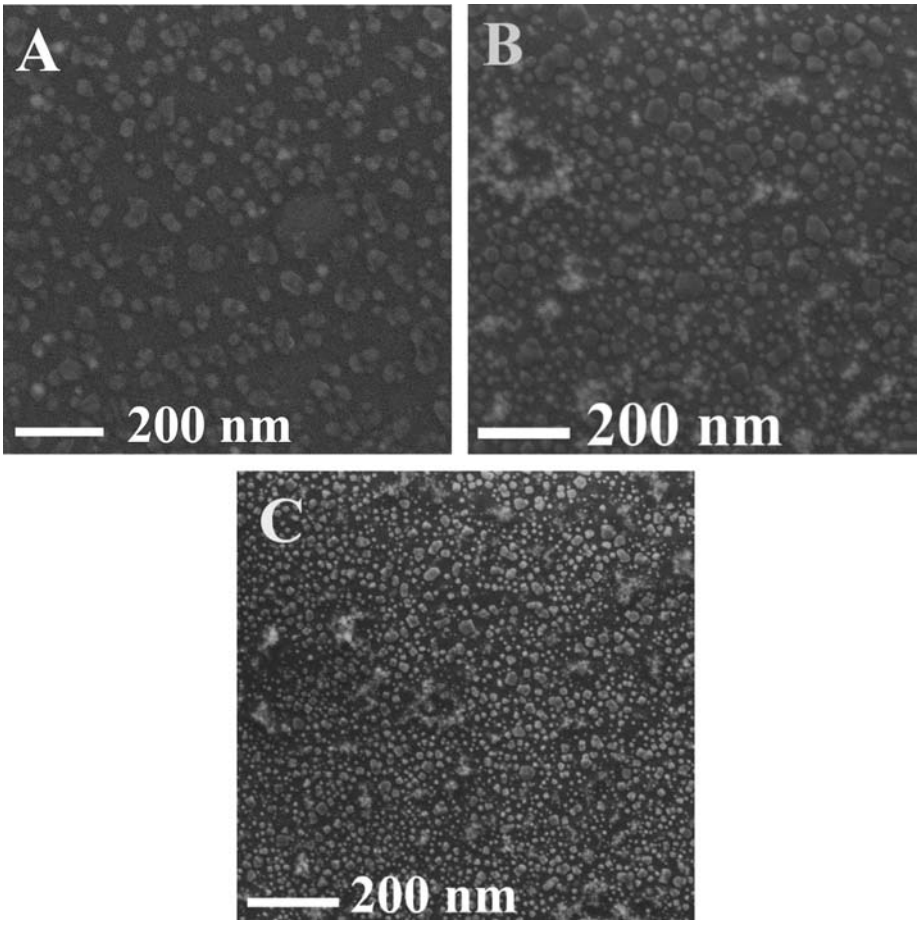


**Fig. 2.** FE-SEM of the hybrid films prepared using different concentrations of $HAuCl_4$. Concentrations of $HAuCl_4$: (A) 1 mmol $L^{-1}$; (B) 3 mmol $L^{-1}$; and (C) 4 mmol $L^{-1}$.

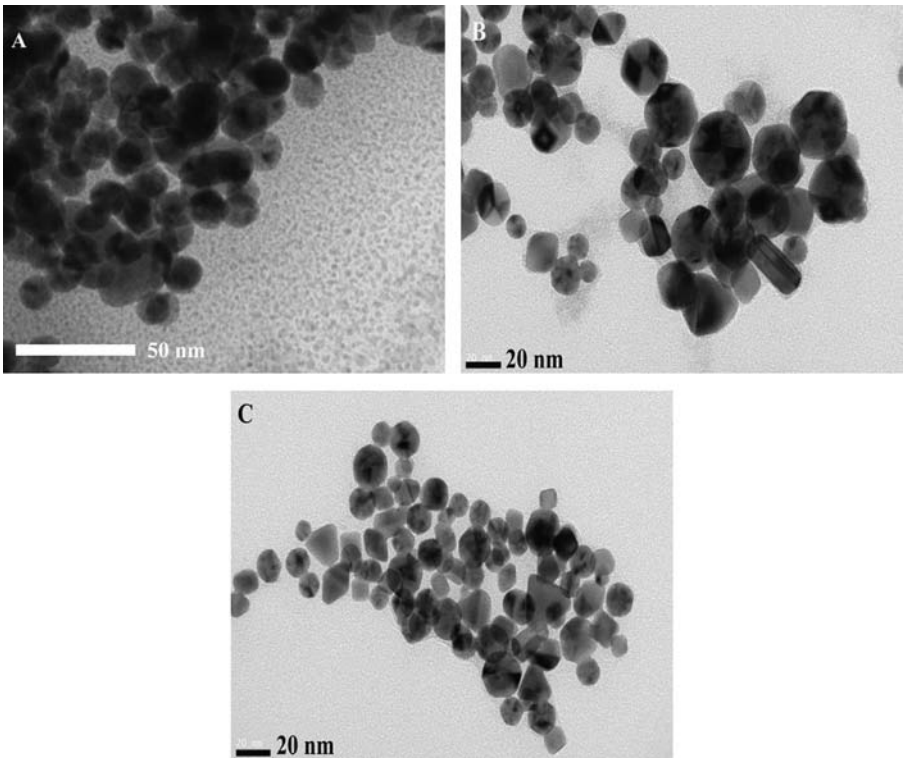


**Fig. 3.** TEM of GNPs prepared using different solutions. (A) Water; (B) CHIT (0.125%, wt%); and (C) CHIT (0.125%, wt %) and IL (5 μL $mL^{-1}$).

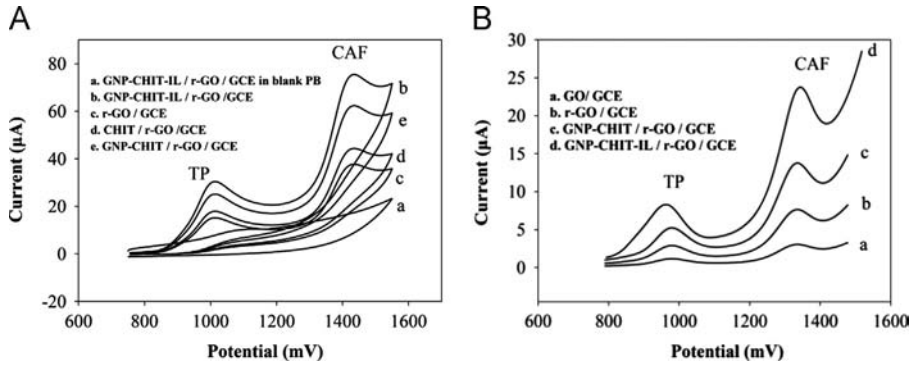


**Fig. 4.** (A) CVs of different electrodes in 0.1 mol $L^{-1}$ PBS (pH 7.4) containing $1.0 \times 10^{-7}$ mol $L^{-1}$ TP and $5.0 \times 10^{-7}$ mol $L^{-1}$ CAF. Electrodes: (b) anisotropic GNP–CHIT–IL/r-GO/GCE; (c) r-GO/ GCE; (d) CHIT/r-GO/GCE; and (e) the anisotropic GNP–CHIT/r-GO/GCE. (a) CV of GNP–CHIT–IL/r-GO/GCE in 0.1 mol $L^{-1}$ PBS (pH 7.4). (B) DPV response of different electrodes in 0.1 mol $L^{-1}$ PBS (pH 7.4) containing $1.0 \times 10^{-7}$ mol $L^{-1}$ TP and $5.0 \times 10^{-7}$ mol $L^{-1}$ CAF. Electrodes: (a) GO/GCE; (b) r-GO/GCE; (c) GNP–CHIT/r-GO/GCE; (d) the anisotropic GNP–CHIT–IL/r-GO/GCE.

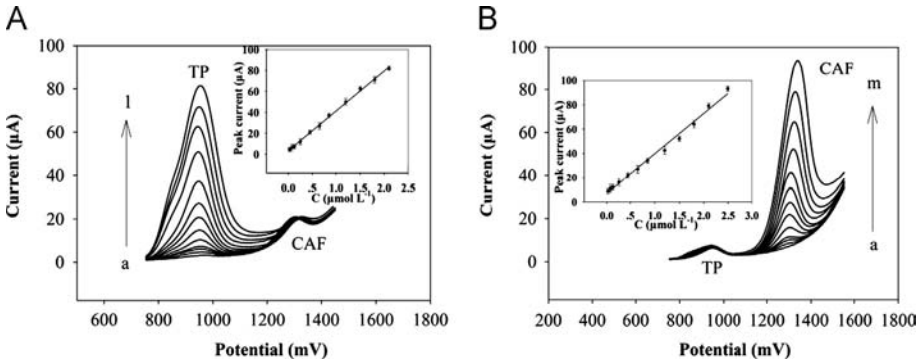


**Fig. 5.** (A) DPVs of the anisotropic GNP–CHIT–IL/r-GO/GCE/r-GO in 0.1 mol $L^{-1}$ PBS(pH 7.4) containing $5.0 \times 10^{-7}$ mol $L^{-1}$ CAF and different concentration of TP. The inset is the calibration curve of TP. (B) DPVs of the anisotropic GNP–CHIT–IL/r-GO/GCE/r-GO in 0.1 mol $L^{-1}$ PBS (pH 7.4) containing $1.0 \times 10^{-7}$ mol $L^{-1}$TP and different concentration of CAF. The inset is the calibration curve of CAF.

30 nm (Fig. 3(c)), which means that IL plays an important role to control the diameter of GNP.

### 3.3. Voltammetric characterization of TP and CAF at different modified electrodes

Electrochemical behavior of TP and CAF at the anisotropic GNP–CHIT–IL/r-GO/GCE is characterized with cyclic voltammetry (CV) (Fig. 4(A)). The electrode exhibits a small background current in a blank PBS. Upon the addition of $1.0 \times 10^{-7}$ mol $L^{-1}$ CAF and $5.0 \times 10^{-7}$ mol $L^{-1}$ TP, two irreversible oxidation peaks appear at 1.05 V and 1.39 V, respectively, which should be attributed to the oxidation of CAF and TP. CV is used to investigate the roles of r-GO, CHIT, IL and anisotropic GNP. The response of CHIT–GO/ GCE is stronger than the r-GO/GCE, which should be attributed to the adsorption of CHIT. The response of anisotropic GNP–CHIT/r-GO/ GCE is better than CHIT–r-GO/GCE because of the electro-catalytic activity of anisotropic GNP. The response of anisotropic GNP–CHIT–IL/r-GO/GCE is obviously enhanced in comparison with the GNP–CHIT/r-GO/GCE, which means IL benefits the accumulation of TP and CAF (Fig. 4).

At the same time, the differential pulse voltammetry (DPV) response of TP and CAF at different modified electrodes is also discussed (Fig. 4(B)). It is found that the response of r-GO modified electrode is stronger than GO/GCE, which is due to the good electric conductivity of r-GO. The response of anisotropic GNP–CHIT/r-GO/GCE is better than r-GO/GCE, meaning that GNP and CHIT can promote the electrochemical process. Furthermore, the response of anisotropic GNP–CHIT–IL/r-GO/GCE is best, which accords with the electrochemical characterization using CV.

### 3.4. Optimization of experimental variables

#### 3.4.1. Effect of r-GO on the response of anisotropic GNP–CHIT–IL/r-GO/GCE to TP and CAF

The response of TP and CAF at the anisotropic GNP–CHIT–IL/r-GO/GCE prepared with various concentrations of r-GO is studied (Fig. S2(A)). The result indicates that the peak currents of TP and CAF increase quickly by increasing the concentration of r-GO coated on GCE surface (0.4–1.0 mg $L^{-1}$), which means the electro-catalytic active sites increase. Further increase causes a gradual decrease, which can be attributed to the increase in film thickness. As a result, 5 μL of 1.0 mg $L^{-1}$ r-GO is selected as optimum volume for preparing the modified electrode.

#### 3.4.2. Effect of IL concentration on the response of anisotropic GNP–CHIT–IL/GCE to TP and CAF

The effect of IL concentration on the response of TP and CAF at the anisotropic GNP–CHIT–IL/r-GO/GCE is investigated in range from 2–8 μL $mL^{-1}$ (Fig. S2(B)). It is clear when the concentration of IL is 5 μL $mL^{-1}$, the modified electrode has the best response for TP and CAF. The result is in accordance with the change of morphology of the hybrid film prepared with different concentrations of IL (see Fig. 1(B)–(E)). The reason should be that when the concentration of IL is too low, the loaded anisotropic GNPs agglomerate so that the film has small surface. On the contrary, when the concentration of IL is too high the hybrid film becomes smooth and presents smaller surface areas in comparison with three-dimensional and rough surface.

*3.4.3. Effect of $HAuCl_4$ concentration on the response of anisotropic GNP–CHIT–IL/r-GO/GCE to TP and CAF*

The effect of $HAuCl_4$ concentration on the response of the anisotropic GNP–CHIT–IL/r-GO/GCE to TP and CAF is researched (Fig. S3(C)). It is obvious that the oxidation current for TP and CAF increases quickly by increasing the concentration of $HAuCl_4$ from 0.5 mmol $L^{-1}$ to 4.0 mmol $L^{-1}$. This is because the quantity of anisotropic GNPs depends on it. However, when the concentration of $HAuCl_4$ exceeds 4.0 mmol $L^{-1}$ the anisotropic GNPs agglomerate in hybrid film. Therefore, the oxidation current gradually decreases.

*3.4.4. Effect of pH on the response of anisotropic GNP–CHIT–IL/r-GO/GCE to TP and CAF*

The influence of pH is investigated over the range of 6.4–8.0 (Fig. S2(D)). Result indicates that the optimum pH is 7.4, which is a suitable condition for the stable existence of CHIT on the electrode surface. Therefore, pH 7.4 is fixed for the experiments. At the same time, the slopes of the peak potential for TP and CAF vs pH plots are about $-50.4$ mV $pH^{-1}$ and $-51$ mV $pH^{-1}$ (data not shown), respectively, which suggests that the number of electrons transfered is equal to that of hydrogen ions taking part in the electrode reaction.

*3.4.5. Effect of accumulation time on the response of anisotropic GNP–CHIT–IL/r-GO/GCE to TP and CAF*

The effect of accumulation time on the oxidation peak current is studied at open circuit potential (Fig. S2(E)). The result indicates that the oxidation peak current increases gradually with extending accumulation time from 0 to 300 s for $1.0\times10^{-7}$ mol $L^{-1}$ TP and $5.0\times10^{-7}$ mol $L^{-1}$ CAF. This can be attributed to the adsorption of TP and CAF on electrode surface. Then, the oxidation peak current tends to level off. This phenomenon can be attributed to the saturated adsorption of TP and CAF. So, 300 s is chosen as accumulation time.

*3.5. The optimal response characteristics of anisotropic GNP–CHIT–IL/r-GO/GCE*

Under optimal experimental conditions, DPVs of TP and CAF solutions with different concentrations are recorded. As expected, the response currents increase upon the increase of TP and CAF concentration. The calibration curves for the detection of TP and CAF are shown in Fig. 5. The linear response range for TP is $2.50\times10^{-8}$–$2.10\times10^{-6}$ mol $L^{-1}$ with a regression equation of $i_p$ ($\mu A$)=3.08+38.10 C (μmol $L^{-1}$), $r$=0.995) (Fig. 5(A)); for CAF it is $2.50\times10^{-8}$–$2.49\times10^{-6}$ mol $L^{-1}$ with a regression equation of $i_p$ ($\mu A$)=6.07+33.06 C (μmol $L^{-1}$, $r$=0.993) (Fig. 5(B)). The detection limits are $1.32\times10^{-9}$ mol $L^{-1}$ (for TP) and $4.42\times10^{-9}$ mol $L^{-1}$ (for CAF) at $3\sigma$, respectively. The performance of GNP–CHIT–IL/r-GO/GCE is compared with other modified electrodes, and the results are listed in Tables S1 and S2 (Supporting information). It can be seen that the anisotropic GNP–CHIT–IL/r-GO/GCE offers a reasonable linear range and the detection limit is lower than most of previous reports except the report for the determination of TP [34].

*3.6. Selectivity*

To assess the selectivity of the anisotropic GNP–CHIT–IL/r-GO/GCE, the interference of some possible inorganic ions and organic compounds in real samples is investigated in the presence of $1.0\times10^{-7}$ mol $L^{-1}$ TP and $5.0\times10^{-7}$ mol $L^{-1}$ CAF. The result indicates that 500-fold of $Cu^{2+}$, $Hg^{2+}$, $Pb^{2+}$, $Mg^{2+}$, $Ca^{2+}$, $Al^{3+}$ and $Fe^{3+}$, and 250 fold of glucose, catechol, ascorbic acid, uric acid, oxalic acid, glutamic acid and lactic acid have no interference to TP and CAF (signal change below 5%).

*3.7. Repeatability and stability*

The repeatability of the anisotropic GNP–CHIT–IL/r-GO/GCE was investigated for responding to $1.0\times10^{-7}$ mol $L^{-1}$ TP and $5.0\times10^{-7}$ mol $L^{-1}$ CAF, and variation coefficients (i.e. RSD) of 6.95% and 5.11% were observed for five successive assays, respectively. The current response of the sensor still remained up to 97.2% and 96.6% of the initial values after 50 successive assays for TP and CAF, respectively. The stability of the electrode was investigated by recording its response to $1.0\times10^{-7}$ mol $L^{-1}$ TP and $5.0\times10^{-7}$ mol $L^{-1}$ CAF over 60 days. When not in use, the electrode was stored at 4 °C under wet environment. After 60 days, the current response of the sensor still remained up to 93.1% (RSD=4.47%, $n$=5) (for TP) and 95.6% (for CAF) (RSD=4.56%, $n$=5) of its initial values respectively. The fabrication reproducibility was also estimated with five different electrodes, which were fabricated independently by the same procedure. The RSDs were 5.8% and 5.1% for the peak currents of $1.0\times10^{-7}$ mol $L^{-1}$ TP and 5.0 $10^{-7}$ mol $L^{-1}$ CAF, respectively, which demonstrates the reliability of the fabrication procedure. These results demonstrate the good repeatability and high stability of the anisotropic GNP–CHIT–IL/r-GO/GCE.

*3.8. Detection of real samples*

Finally, the proposed electrochemical sensor was evaluated by performing tests of TP and CAF in real samples including tea, energy drink and pharmaceutics (Table 1(a)). Green tea ( Pu'er Tea) (5.0 g ) was finely powdered in an mortar, and dissolved in 150 mL redistilled water at 60 °C for 5 h. The obtained mixture was filtered with a membrane filter, and then was determined under the optimized conditions. Ten theophylline sustained-release tablets were accurately weighed and triturated. 100 mg of the resulted powder was dissolved and transferred into a 100 mL calibrated flask and completed to the volume with double distilled water. Akafen powder samples were prepared using the similar method. The results are shown in Table 1, which agree with the results

**Table 1**
Detection results of real samples.

| Samples | Found by HPLC (μmol $L^{-1}$) | | Determined by this method (μmol $L^{-1}$) | | RSD (%, $n$=5) | |
|---|---|---|---|---|---|---|
| | TP | CAF | TP | CAF | TP | CAF |
| Green tea | 0.23 | 2.46 | 0.20 | 2.44 | 6.7 | 5.1 |
| Pu'er tea | 0.26 | 2.21 | 0.23 | 2.25 | 3.9 | 4.4 |
| Energy drink | 0.00 | 1.13 | 0.00 | 1.06 | | 6.2 |
| Theophylline tablet | 2.02 | 0.00 | 2.08 | 0.00 | 3.2 | |
| Akafen powder | 0.00 | 1.29 | 0.00 | 1.31 | | 6.7 |

**Table 2**
Recovery tests for TP and CAF added in human urine and serum samples.

| Sample | Added (μmol $L^{-1}$) | | Found (μmol $L^{-1}$) | | Recovery (%) | | RSD (%, $n$=5) | |
|---|---|---|---|---|---|---|---|---|
| | TP | CAF | TP | CAF | TP | CAF | TP | CAF |
| Urine | 0.15 | 0.50 | 0.145 | 0.48 | 97 | 96 | 4.3 | 5.6 |
| | 0.30 | 1.00 | 0.282 | 1.01 | 94 | 101 | 3.2 | 5.2 |
| | 1.00 | 1.50 | 1.07 | 1.54 | 107 | 103 | 5.1 | 4.2 |
| Serum | 0.15 | 0.50 | 0.155 | 0.52 | 103 | 104 | 4.2 | 6.1 |
| | 0.30 | 1.00 | 0.303 | 1.05 | 101 | 105 | 5.0 | 4.6 |
| | 1.00 | 1.50 | 1.03 | 1.47 | 103 | 98 | 4.1 | 3.1 |

obtained by HPLC. The proposed electrochemical sensor was evaluated by performing recovery tests for TP and CAF in human serum samples and urine samples (Table 2). The recoveries for the TP and CAF standards added are 97% to 107% and 98% to 104%, respectively.

## 4. Conclusions

In this paper, a solution approach for preparing the hybrid solution of anisotropic GNP–CHIT–IL is developed. Here, CHIT makes gold form anisotropic structure, and IL plays a role to control the diameter of GNP and the structure of hybrid film. An electrochemical sensor is constructed by directly coating the hybrid solution on r-GO modified GCE. The hybrid film has a three-dimensional structure, and small anisotropic GNPs are well dispersed in it. This sensor shows a sensitive and selective response to TP and CAF. It also has the advantages of simple, low-cost and effective. This work provides a useful platform for rapidly preparing anisotropic metallic nanoparticles hybrid based sensors.

## Acknowledgments

This work was jointly supported by the National Natural Science Foundation of China (Grant nos. 21075092 and 21277105) and the Youth Foundation of Science Commission of Yunnan Province (Grant no. 2012FD061).

## Appendix A. Supporting information

Supplementary data associated with this article can be found in the online version at http://dx.doi.org/10.1016/j.talanta.2014.03.029.

## References

[1] E.C. Dreaden, A.M. Alkilany, X. Huang, C.J. Murphy, M.A. El-Sayed, Chem. Soc. Rev. 41 (2012) 2740–2779.
[2] A. Tiwari, M. Ramalingam, H. Kobayashi, A.P. Turner, Biomedical Materials and Diagnostic Devices, Wiley-Scrivener, USA, 2012.
[3] A. Tiwari, A.P.F. Turner, Biosensors Nanotechnology, Wiley-Scrivener, USA, 2014.
[4] K. Okitsu, Y. Mizukoshi, T.A. Yamamoto, Y. Maeda, Y. Nagata, Mater. Lett. 61 (2007) 3429–3431.
[5] S. Guo, E. Wang, Anal. Chim. Acta 598 (2007) 181–192.
[6] Z. Li, Z. Liu, J. Zhang, B. Han, J. Du, Y. Gao, T. Jiang, J. Phys. Chem. B 109 (2005) 14445–14448.
[7] J. Zhu, Y. Shen, A. Xie, L. Qiu, Q. Zhang, S. Zhang, J. Phys. Chem. B 111 (2007) 7629–7633.
[8] T. Tsuda, S. Seino, S. Kuwabata, Chem. Commun. (2009) 6792–6794.
[9] G. Yang, F. Zhao, B. Zeng, Biosens. Bioelectron. 53C (2013) 447–452.
[10] Y. Jin, Z. Li, L. Hu, X. Shi, W. Guan, Y. Du, Carbohydr. Polym. 91 (2013) 152–156.
[11] F. Spano, A. Massaro, L. Blasi, M. Malerba, R. Cingolani, A. Athanassiou, Langmuir 28 (2012) 3911–3917.
[12] G. Di Carlo, A. Curulli, R.G. Toro, C. Bianchini, T. de Caro, G. Padeletti, D. Zane, G. M. Ingo, Langmuir 28 (2012) 5471–5479.
[13] P.A. Mitenko, R.I. Ogilvie, N. Engl. J. Med. 289 (1973) 600–603.
[14] V. Bellia, S. Battaglia, M.G. Matera, M. Cazzola, Pulm. Pharmacol. Ther. 19 (2006) 311–319.
[15] A. Nehlig, J.L. Daval, G. Debry, Brain Res. Rev. 17 (1992) 139–170.
[16] M.K. McMullen, J.M. Whitehouse, G. Shine, A. Towell, Food Funct. 2 (2011) 197–203.
[17] S. Kerrigan, T. Lindsey, Forensic Sci. Int. 153 (2005) 67–69.
[18] C.W. Huck, W. Guggenbichler, G.K. Bonn, Anal. Chim. Acta 538 (2005) 195–203.
[19] J.W. Dove, G. Buckton, C. Doherty, Int. J. Pharm. 138 (1996) 199–206.
[20] S. Nafisi, D.S. Shamloo, N. Mohajerani, A. Omidi, J. Mol. Struct. 608 (2002) 1–7.
[21] Y.H. Zhu, Z.L. Zhang, D.W. Pang, J. Electroanal. Chem. 581 (2005) 303–309.
[22] L. Liu, F. Xiao, J. Li, W. Wu, F. Zhao, B. Zeng, Electroanalysis 20 (2008) 1194–1199.
[23] T. Alizadeh, M.R. Ganjali, M. Zare, P. Norouzi, Electrochim. Acta 55 (2010) 1568–1574.
[24] Y. Gao, H. Wang, L. Guo, J. Electroanal. Chem. 706 (2013) 7–12.
[25] S. Yang, R. Yang, G. Li, L. Qu, J. Li, L. Yu, J. Electroanal. Chem. 639 (2010) 77–82.
[26] J.Y. Sun, K.J. Huang, S.Y. Wei, Z.W. Wu, F.P. Ren, Colloids Surf. B 84 (2011) 421–426.
[27] R.N. Goyal, S. Bishnoi, B. Agrawal, J. Electroanal. Chem. 655 (2011) 97–102.
[28] S.J. Malode, N.P. Shetti, S.T. Nandibewoor, Colloids Surf. B 97 (2012) 1–6.
[29] W.D.J.R. Santos, M. Santhiago, I.V.P. Yoshida, L.T. Kubota, Sens. Actuators B 166–167 (2012) 739–745.
[30] Y. Li, S. Wu, P. Luo, J. Liu, G. Song, K. Zhang, B. Ye, Anal. Sci. 28 (2012) 497–502.
[31] V.K. Gupta, A.K. Jain, S.K. Shoora, Electrochim. Acta 93 (2013) 248–253.
[32] F. Cui, X. Zhang, J. Solid State Electrochem. 17 (2012) 167–173.
[33] G.C. Zhao, X. Yang, Electrochem. Commun. 12 (2010) 300–302.
[34] L. Zi, J. Li, Y. Mao, R. Yang, L. Qu, Electrochim. Acta 78 (2012) 434–439.
[35] S. Guo, Q. Zhu, B. Yang, J. Wang, B. Ye, Food Chem. 129 (2011) 1311–1314.
[36] M. Amare, S. Admassie, Talanta 93 (2012) 122–128.
[37] C.A. Martínez-Huitle, N. Suely Fernandes, S. Ferro, A. De Battisti, M.A. Quiroz, Diam. Relat. Mater. 19 (2010) 1188–1193.
[38] L. Svorc, P. Tomcik, J. Svitkova, M. Rievaj, D. Bustin, Food Chem. 135 (2012) 1198–1204.
[39] H. Yin, X. Meng, H. Su, M. Xu, S. Ai, Food Chem. 134 (2012) 1225–1230.
[40] C. Tan, X. Huang, H. Zhang, Mater. Today 16 (2013) 29–36.
[41] A. Tiwari, Adv. Mat. Lett. 3 (2012) 172–173.
[42] J. Tyagi, R. Kakkar, Adv. Mat. Lett. 4 (2013) 721.
[43] M. Muralidharan, S. Ansari, Adv. Mat. Lett. 4 (2013) 6.
[44] O. Parlak, A. Tiwari, A.P. Turner, A. Tiwari, Biosens. Bioelectron. 49 (2013) 53–62.
[45] A. Chaturvedi, A. Tiwari, A. Tiwari, Adv. Mat. Lett. 4 (2013).
[46] O. Parlak, A.P.F. Turner, A. Tiwari, Adv. Mater. 26 (2014) 482–486.
[47] Y. Liang, D. Wu, X. Feng, K. Müllen, Adv. Mater. 21 (2009) 1679–1683.
[48] K. Ma, H. Wang, M. Zhao, J. Xing, Anal. Chim. Acta 650 (2009) 227–233.
[49] X. Zeng, X. Li, L. Xing, X. Liu, S. Luo, W. Wei, B. Kong, Y. Li, Biosens. Bioelectron. 24 (2009) 2898–2903.
[50] A.I. Gopalan, K.P. Lee, D. Ragupathy, Biosens. Bioelectron. 24 (2009) 2211–2217.
[51] L. Wang, W. Wen, H. Xiong, X. Zhang, H. Gu, S. Wang, Anal. Chim. Acta 758 (2013) 66–71.